The velocity distribution of water molecules ...

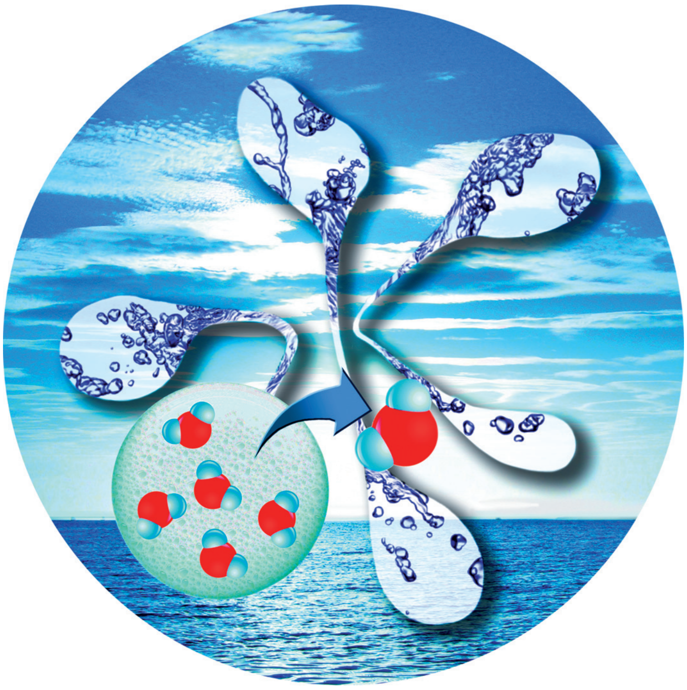

… evaporated from a mass-selected protonated water nanodroplet after a collision-induced electronic excitation is reported. In their Communication on page 14685 ff., M. Farizon et al. show that besides the Maxwell–Boltzmann statistics behavior, a distinct high-velocity contribution provides evidence for molecular evaporation before complete energy redistribution, corresponding to non-ergodic events.

How to contact us:

Editorial Office:
E-mail: angewandte@wiley-vch.de
Fax: (+49) 6201–606-331
Telephone: (+49) 6201–606-315

Reprints, E-Prints, Posters, Calendars:
Carmen Leitner
E-mail: chem-reprints@wiley-vch.de
Fax: (+49) 6201–606-331
Telephone: (+49) 6201–606-327

Copyright Permission:
Bettina Loycke
E-mail: rights-and-licences@wiley-vch.de
Fax: (+49) 6201–606-332
Telephone: (+49) 6201–606-280

Online Open:
Margitta Schmitt
E-mail: angewandte@wiley-vch.de
Fax: (+49) 6201–606-331
Telephone: (+49) 6201–606-315

Subscriptions:
www.wileycustomerhelp.com
Fax: (+49) 6201–606-184
Telephone: 0800 1800536 (Germany only)
+44(0) 1865476721 (all other countries)

Advertising:
Marion Schulz
E-mail: mschulz@wiley-vch.de
Fax: (+49) 6201–606-550
Telephone: (+49) 6201–606-565

Courier Services:
Boschstrasse 12, 69469 Weinheim

Regular Mail:
Postfach 101161, 69451 Weinheim

Angewandte Chemie International Edition is a journal of the Gesellschaft Deutscher Chemiker (GDCh), the largest chemistry-related scientific society in continental Europe. Information on the various activities and services of the GDCh, for example, cheaper subscription to *Angewandte Chemie International Edition*, as well as applications for membership can be found at **www.gdch.de** or can be requested from GDCh, Postfach 900440, D-60444 Frankfurt am Main, Germany.

GDCh
Gesellschaft
Deutscher Chemiker

Biosynthesis
In their Communication on page 14660 ff., A. Schaller, Q. Wang, and co-workers report that the dirigent protein GhDIR4 is responsible for the atropselective biosynthesis of (+)-gossypol (see structure) in cotton plants (*Gossypium hirsutum*).

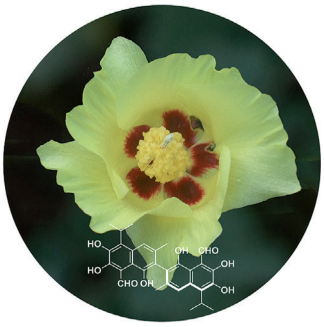

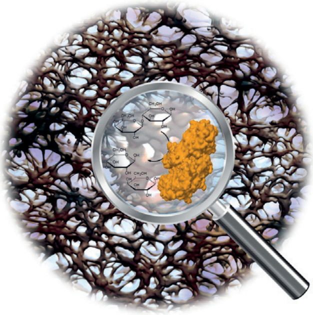

Membranes
Tailor-made biocatalysts are immobilized on polymeric filtration membranes. In their Communication on page 14800 ff., P. Shahgaldian et al. show that the immobilization is stable, but reversible.

Cycloaddition Reactions
In their Communication on page 14849 ff., J. Zhang et al. describe the first example of a gold(I)-catalyzed intermolecular annulation of *N*-allenamides at the proximal C=C bond.

Service

Author Profile

*“I can never resist a slice of cream cake.
My favorite author (fiction) is E. T. A. Hoffmann …”*
This and more about Robert Häner can be found on page 14616.

News

G. K. S. Prakash

C. Chizallet

S. K. Bhargava

Books

Highlights

Antiparasitics

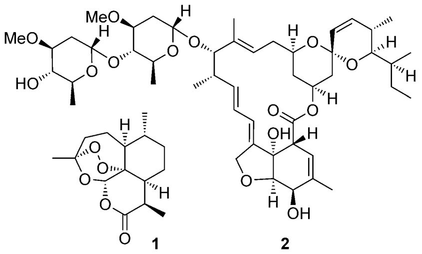

An end to suffering: Parasitic infections with protozoa and worms cause unimaginable misery, in particular in the tropics. Fortunately, natural products, such as the antimalarial artemisinin (**1**) and the anthelmintic avermectin (**2**) were discovered and developed into therapeutics. These major achievements now culminated in the 2015 Nobel Prize for Medicine.

Minireviews

Polymer Dots

Emission enhancement of non-fluorophore units (called sub-fluorophores) by crosslinking them (crosslink-enhanced emission; CEE) is utilized in a new type of fluorescent material: non-conjugated polymer dots (NCPDs). The CEE can be covalently bonded, rigidity aggregated, or supramolecular in nature. The synthetic strategies, optical properties, and potential applications of NCPDs in biology-related fields are discussed.

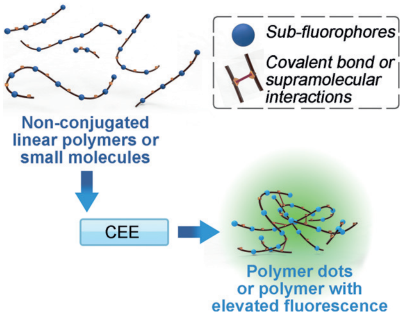

Reviews

Quinone Catalysis

Quinones are highly useful reagents for the dehydrogenation and oxidative functionalization of organic molecules, but they are often used in stoichiometric quantities. This Review highlights recent advances in quinone-catalyzed reactions wherein the reduced quinone is regenerated by a more-desirable stoichiometric oxidant. In many cases, O_2 is capable of serving as the terminal oxidant (see scheme; Sub = substrate).

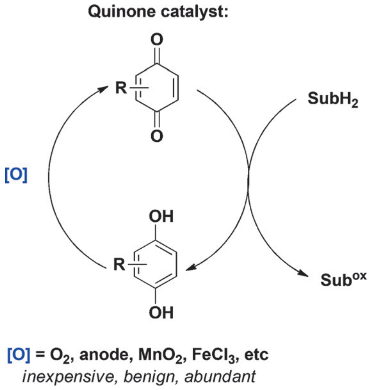

For the USA and Canada:
ANGEWANDTE CHEMIE International Edition (ISSN 1433-7851) is published weekly by Wiley-VCH, PO Box 101161, 69451 Weinheim, Germany. US mailing agent: SPP, PO Box 437, Emigsville, PA 17318. Periodicals postage paid at Emigsville, PA. US POSTMASTER: send address changes to *Angewandte Chemie*, John Wiley & Sons Inc., C/O The Sheridan Press, PO Box 465, Hanover, PA 17331. Annual subscription price for institutions: US$ 11.738/10.206 (valid for print and electronic / print or electronic delivery); for individuals who are personal members of a national chemical society prices are available on request. Postage and handling charges included. All prices are subject to local VAT/sales tax.

Communications

Biosynthesis

I. Effenberger, B. Zhang, L. Li, Q. Wang,
Y. Liu, I. Klaiber, J. Pfannstiel, Q. Wang,*
A. Schaller* ______ 14660 – 14663

Dirigent Proteins from Cotton (*Gossypium* sp.) for the Atropselective Synthesis of Gossypol

Frontispiece

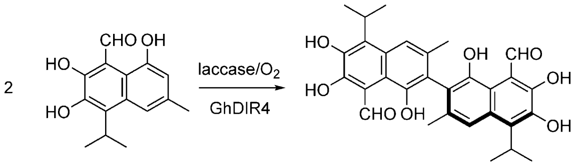

Protein at the helm: The dirigent protein GhDIR4 is responsible for the atropselective biosynthesis of (+)-gossypol in cotton (*Gossypium hirsutum*) plants. GhDIR4 also confers atropselectivity to the oxidative coupling of hemigossypol in vitro. Cotton dirigent proteins have potential as tools for the asymmetric synthesis of axially chiral binaphthyls.

Model Membranes

T. Zapf, C.-W. D. Tan, T. Reinelt, C. Huber,
D. Shaohua, S. Geifman-Shochat,
H. Paulsen, E.-K. Sinner* 14664 – 14668

Synthesis and Functional Reconstitution of Light-Harvesting Complex II into Polymeric Membrane Architectures

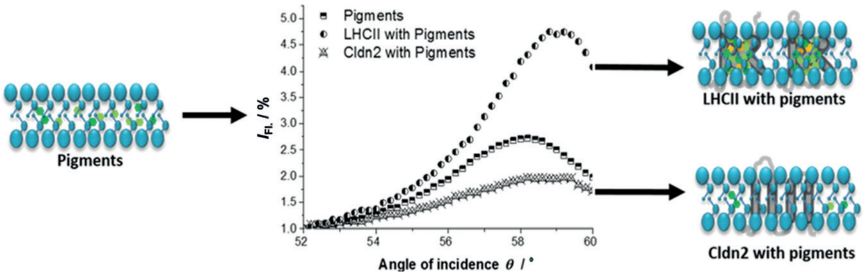

Designed to catch the light: Light-harvesting complex II (LHCII) is one of the most abundant and best studied membrane proteins in the world. The integration of LHCII into polymeric membranes through cell-free protein synthesis offers a means to overcome random insertion and other technological limitations of lipid or detergent-based arrays for LHC-based light harvesting.

Amyloids

T. Schubeis, P. Yuan, M. Ahmed,
M. Nagaraj, B.-J. van Rossum,
C. Ritter* ______ 14669 – 14672

Untangling a Repetitive Amyloid Sequence: Correlating Biofilm-Derived and Segmentally Labeled Curli Fimbriae by Solid-State NMR Spectroscopy

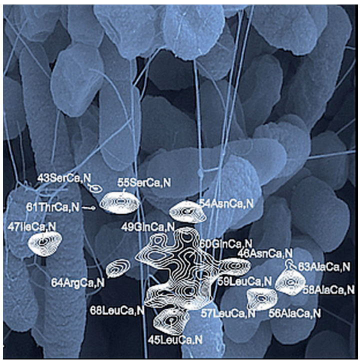

It's a marvel of bacterial engineering: Amyloids are known for their structural polymorphisms, which hampers gaining a mechanistic understanding of their role in diseases. Bacteria produce the functional amyloid curli to form biofilms. Solid-state NMR spectroscopy of biofilm-derived and recombinant curli reveals a well-defined, highly resilient conformation. Segmental isotope labeling allows a first indication of its structural features.

Microporous Materials

A. C. Uptmoor, J. Freudenberg,
S. T. Schwäbel, F. Paulus, F. Rominger,
F. Hinkel, U. H. F. Bunz* 14673 – 14676

Reverse Engineering of Conjugated Microporous Polymers: Defect Structures of Tetrakis(4-ethynylphenyl)stannane Networks

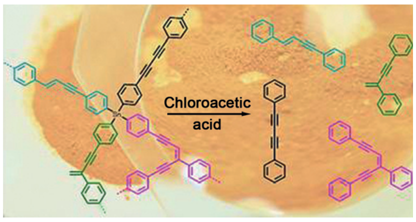

Burn your bridges: Two different conjugated microporous polymers (CMPs) based on tetrakis(4-ethynylphenyl)stannane as the repeating unit were synthesized and characterized. Selective cleavage of the tin–carbon bonds with chloroacetic acid affords the isolated bridging units, thereby providing insight into the structure of the organic linkers and the surprisingly varied chemical composition of these networks.

Tyrosinase

A. Bijelic, M. Pretzler, C. Molitor, F. Zekiri,
A. Rompel* ______________ **14677 – 14680**

The Structure of a Plant Tyrosinase from Walnut Leaves Reveals the Importance of "Substrate-Guiding Residues" for Enzymatic Specificity

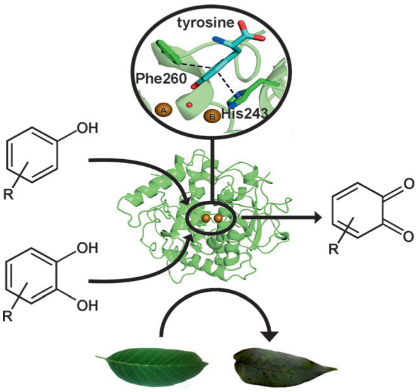

Identity crisis: The first plant tyrosinase structure was solved by the means of X-ray crystallography and reveals that, according to an early theory, this tyrosinase should rather be a catechol oxidase. However, its tyrosinase identity was confirmed by kinetic studies. A binding mechanism is suggested that explains its activity despite its catechol-oxidase-like structure.

Crystallization

J. Anwar,* S. Khan,
L. Lindfors ______________ **14681 – 14684**

Secondary Crystal Nucleation: Nuclei Breeding Factory Uncovered

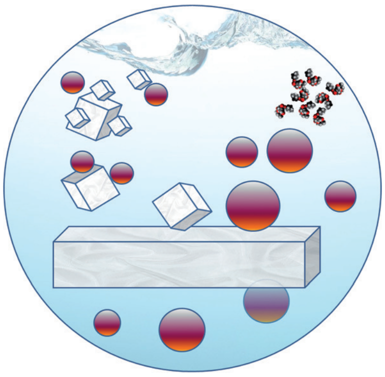

Crystal clear: Molecular dynamics simulations uncover the nuclei breeding factory responsible for secondary nucleation in crystal growth. The question why a few crystal seeds give rise to a many-fold increase in new crystals is answered. This mechanistic insight will enable better control in engineering crystalline products to design.

Molecular Dynamics

H. Abdoul-Carime, F. Berthias,
L. Feketeová, M. Marciante, F. Calvo,
V. Forquet, H. Chermette, B. Farizon,
M. Farizon,* T. D. Märk __ **14685 – 14689**

Velocity of a Molecule Evaporated from a Water Nanodroplet: Maxwell–Boltzmann Statistics versus Non-Ergodic Events

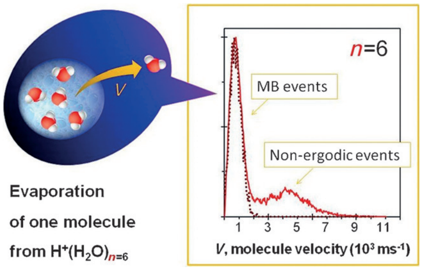

The velocity of molecules evaporated from a mass-selected protonated water nanodroplet is measured event by event using velocity map imaging in combination with a mass spectrometry technique. Besides the Maxwell–Boltzmann (MB) statistics behavior, a distinct high-velocity contribution provides evidence of molecular evaporation before complete energy redistribution, corresponding to non-ergodic events.

Front Cover

Topochemical Polymerization

H. Jin, C. N. Young, G. P. Halada,
B. L. Phillips,
N. S. Goroff* ______________ **14690 – 14695**

Synthesis of the Stable Ordered Conjugated Polymer Poly(dibromodiacetylene) from an Explosive Monomer

Defusing: The reactivity of highly unstable dibromobutadiyne can be controlled by forming cocrystals with oxalamides at low temperature. Topochemical polymerization of dibromobutadiyne monomers leads to the first conjugated polymer containing bromine substituents on the backbone.

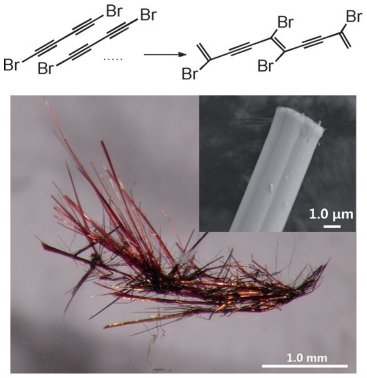

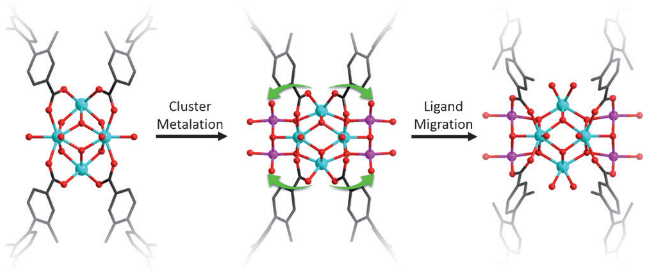

Mixed metal MOF: Cooperative cluster metalation and ligand migration were performed on a Zr-MOF, leading to the isolation of Zr_6M_4 based bimetallic MOFs (right). This strategy allows for the functionalization of Zr-MOFs with other metals for a variety of promising applications.

Metal–Organic Frameworks

S. Yuan, Y.-P. Chen, J. Qin, W. Lu,*
X. Wang, Q. Zhang, M. Bosch, T.-F. Liu,
X. Lian, H.-C. Zhou* ____ **14696 – 14700**

Cooperative Cluster Metalation and Ligand Migration in Zirconium Metal–Organic Frameworks

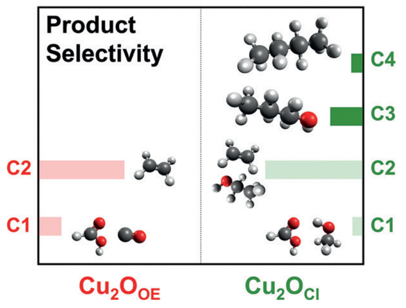

Cl-induced bi-phasic Cu_2O–Cu shows remarkable catalytic ability for CO_2 conversion toward high-carbon-number compounds. The oxidized Cu phase allows reaction intermediates to stay for a longer time on the surface, and consequently leads to formation of larger molecules.

CO_2 Conversion

S. Lee, D. Kim, J. Lee* ____ **14701 – 14705**

Electrocatalytic Production of C3-C4 Compounds by Conversion of CO_2 on a Chloride-Induced Bi-Phasic Cu_2O-Cu Catalyst

Homoleptic nickel(I) complex: A solvent-free organometallic nickel(I) complex was easily obtained from the reaction between $[Ni^0(cod)_2]$ and $Ag[Al(OR^F)_4]$ (cod = 1,5-cyclooctadiene, $OR^F = OC(CF_3)_3$). Crystal-structure analysis, EPR spectroscopy, XANES, and cyclic voltammetry confirmed the salt to be $[Ni(cod)_2]^+[Al(OR^F)_4]^-$, a good starting material for the synthesis of other cationic Ni^I complexes.

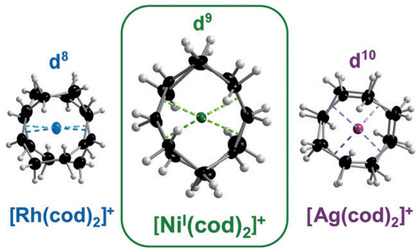

Coordination Modes

M. M. Schwab, D. Himmel, S. Kacprzak,
D. Kratzert, V. Radtke, P. Weis, K. Ray,
E.-W. Scheidt, W. Scherer, B. de Bruin,
S. Weber, I. Krossing* ____ **14706 – 14709**

$[Ni(cod)_2][Al(OR^F)_4]$, a Source for Naked Nickel(I) Chemistry

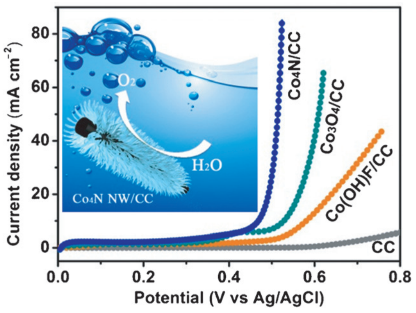

Metallic Co_4N porous nanowire arrays activated by surface oxidation are shown to be highly efficient OER electrocatalysts. Benefiting from multiple synergistic effects of metallic character, 1D porous nanowire structure, and unique 3D electrode configuration, Co_4N NW/CC achieves the best OER performance among well-developed Co-based electrocatalysts to date.

Electrocatalysts

P. Chen, K. Xu, Z. Fang, Y. Tong, J. Wu,
X. Lu, X. Peng, H. Ding, C. Wu,*
Y. Xie ____ **14710 – 14714**

Metallic Co_4N Porous Nanowire Arrays Activated by Surface Oxidation as Electrocatalysts for the Oxygen Evolution Reaction

Protein Modification

J. Fuhrmann,* V. Subramanian,
P. R. Thompson* ________ **14715 – 14718**

Synthesis and Use of a Phosphonate Amidine to Generate an Anti-Phosphoarginine-Specific Antibody

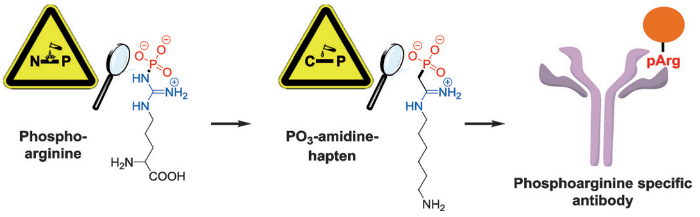

Arginine phosphorylation: Synthesis of stable phosphoarginine analogues enabled the generation of high-affinity sequence-independent anti-phosphoarginine antibodies. These antibodies can be used to directly detect and isolate arginine-phosphorylated proteins.

DNA

K. Röttger, H. J. B. Marroux, M. P. Grubb,
P. M. Coulter, H. Böhnke,
A. S. Henderson, M. C. Galan, F. Temps,*
A. J. Orr-Ewing,*
G. M. Roberts* ________ **14719 – 14722**

Ultraviolet Absorption Induces Hydrogen-Atom Transfer in G·C Watson–Crick DNA Base Pairs in Solution

Inside Cover

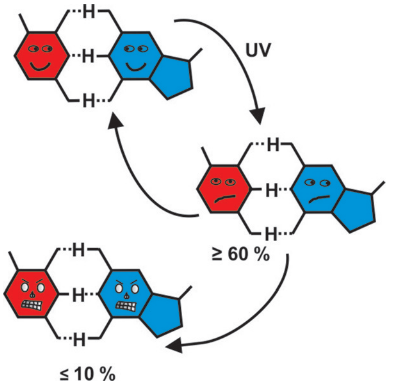

Ultrafast energy-dissipation processes after UV absorption render DNA intrinsically photostable. One of the most debated mechanisms in individual guanine–cytosine base pairs has been confirmed: A sequence of hydrogen transfers across the hydrogen bonds in the dimer lead to an efficient relaxation of the base pair back to the original structure, but up to 10% of the excited molecules instead form a potentially mutagenic tautomer.

Electrocatalysis

R. Ma, Y. Zhou, Y. Chen, P. Li, Q. Liu,
J. Wang* ________ **14723 – 14727**

Ultrafine Molybdenum Carbide Nanoparticles Composited with Carbon as a Highly Active Hydrogen-Evolution Electrocatalyst

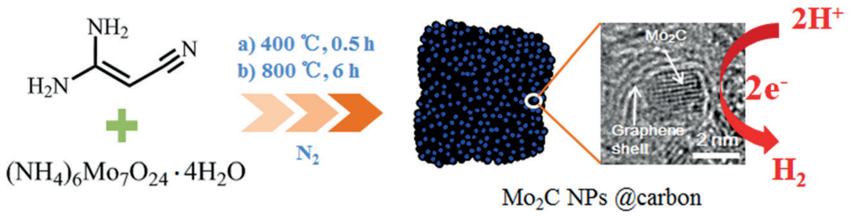

A step is all it takes: A nanocomposite of uniform, ultrafine Mo_2C nanoparticles (NPs) encapsulated by ultrathin graphene shells was synthesized simply by the one-step annealing of a mixture of low-cost dicyanamide and ammonium molybdate (see picture). The resulting material served as a hydrogen-evolving electrocatalyst with excellent activity and long-term stability.

Sensors

E. Roussakis, Z. Li, N. H. Nowell,
A. J. Nichols, C. L. Evans* **14728 – 14731**

Bright, "Clickable" Porphyrins for the Visualization of Oxygenation under Ambient Light

Red light, green light: A group of oxygen-sensitive, "clickable" metalloporphyrins are bright enough to be seen by the naked eye in the absence of oxygen under ambient light. To demonstrate the ease of use of these sensors, one porphyrin was "clicked" into a biocompatible dendrimer, embedded in a bandage formulation, and used to transdermally map oxygen consumption in a burn model.

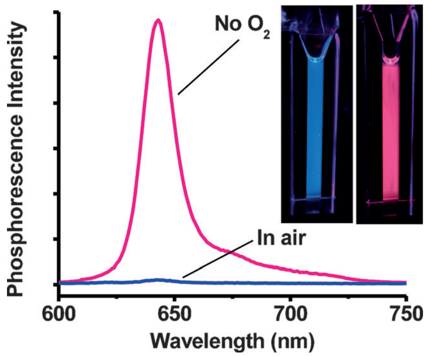

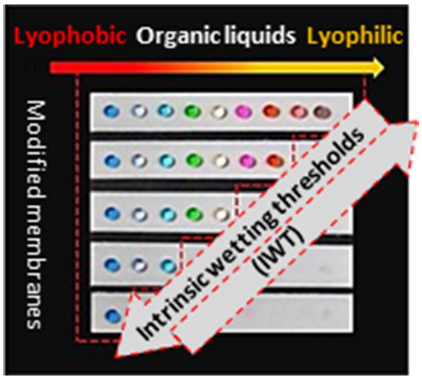

Going separate ways: The surface tensions of nanofibrous membranes have been manipulated to lie in between the intrinsic wetting thresholds (IWTs) of the two organic liquids to be separated. This endows the nanofibrous membranes with superlyophobicity and superlyophilicity for the two liquids, respectively, and thus leads to a successful separation.

Separation of Organic Liquids

L. Wang, Y. Zhao, Y. Tian,*
L. Jiang* ______ **14732 – 14737**

A General Strategy for the Separation of Immiscible Organic Liquids by Manipulating the Surface Tensions of Nanofibrous Membranes

---

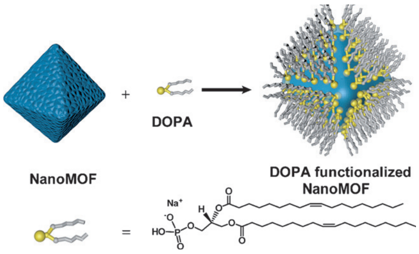

Zr-based MOF nanoparticles densely surface-modified with 1,2-dioleoyl-*sn*-glycero-3-phosphate (DOPA) showed dramatically altered colloidal properties. Post-synthetic modifications can thus be used to modify nanoMOF surface chemistry by coordination to exposed metal-containing units, while retaining crystallinity and permanent porosity.

Surface Functionalization

S. Wang, W. Morris, Y. Liu, C. M. McGuirk, Y. Zhou, J. T. Hupp, O. K. Farha,
C. A. Mirkin* ______ **14738 – 14742**

Surface-Specific Functionalization of Nanoscale Metal–Organic Frameworks

---

Superexchange Tunneling: Self-assembled monolayers (SAMs) of oligoglycines ((Gly)$_n$, $n = 0$–5) are more conductive by tunneling than are SAMs of alkanethiolates. This difference is quantified experimentally and theoretically. Density functional calculations identify the details of the orbitals and electronic couplings involved in superexchange tunneling.

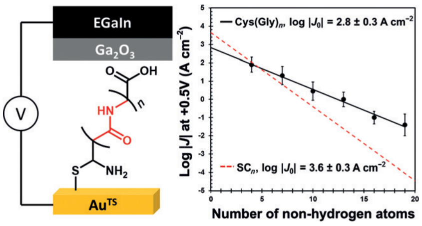

Charge Transport Mechanisms

M. Baghbanzadeh, C. M. Bowers, D. Rappoport, T. Żaba, M. Gonidec, M. H. Al-Sayah, P. Cyganik, A. Aspuru-Guzik,*
G. M. Whitesides* ______ **14743 – 14747**

Charge Tunneling along Short Oligoglycine Chains

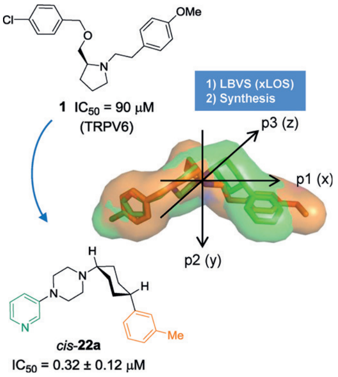

A pharmacophore similarity algorithm called xLOS was used in combination with chemical synthesis to entirely change the scaffold of a weak, unselective inhibitor of calcium channel TRPV6 to obtain a potent, selective inhibitor. Inhibition of TRPV6 selectively reduced cancer cell growth. This virtual screening method may be generally useful to develop tool compounds for poorly characterized targets.

Computer-Aided Drug Design

C. Simonin, M. Awale, M. Brand, R. van Deursen, J. Schwartz, M. Fine, G. Kovacs, P. Häfliger, G. Gyimesi, A. Sithampari, R.-P. Charles, M. A. Hediger,*
J.-L. Reymond* ______ **14748 – 14752**

Optimization of TRPV6 Calcium Channel Inhibitors Using a 3D Ligand-Based Virtual Screening Method

Biomaterials

J. Park, P. Du, J.-K. Jeon, G. H. Jang,
M. P. Hwang, H.-S. Han, K. Park,
K. H. Lee, J.-W. Lee, H. Jeon, Y.-C. Kim,
M. D. J. W. Park, H.-K. Seok,
M.-R. Ok* ______ **14753 – 14757**

Magnesium Corrosion Triggered Spontaneous Generation of H_2O_2 on Oxidized Titanium for Promoting Angiogenesis

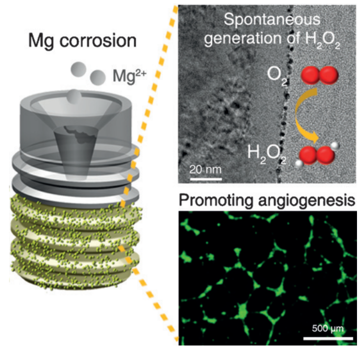

Useful corrosion: An electrochemical system consisting of a biodegradable metal (Mg) and an oxygen-reduction-reaction catalyst was developed for spontaneous H_2O_2 generation. The controlled release of H_2O_2 promoted in vitro angiogenesis in the absence of any growth factors. A conventional titanium implant functionalized by simple magnesium incorporation thus also supports angiogenesis.

Imaging Agents

S. Diao, J. L. Blackburn, G. Hong,
A. L. Antaris, J. Chang, J. Z. Wu, B. Zhang,
K. Cheng, C. J. Kuo,
H. Dai* ______ **14758 – 14762**

Fluorescence Imaging In Vivo at Wavelengths beyond 1500 nm

Semiconducting single-walled carbon nanotubes with large diameters were used for in vivo fluorescence imaging in the long-wavelength near-infrared region (1500–1700 nm). With this imaging agent, 3–4 μm wide capillary blood vessels at a depth of about 3 mm in living mice could be resolved, and the blood-flow speeds in multiple individual vessels were mapped simultaneously.

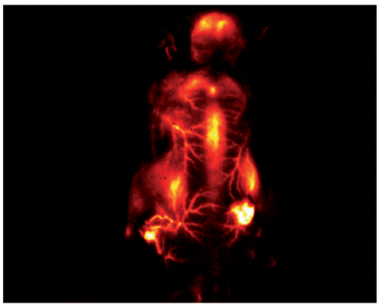

Metalloenzymes

J. M. Bradley, D. A. Svistunenko,
T. L. Lawson, A. M. Hemmings,
G. R. Moore,
N. E. Le Brun* ______ **14763 – 14767**

Three Aromatic Residues are Required for Electron Transfer during Iron Mineralization in Bacterioferritin

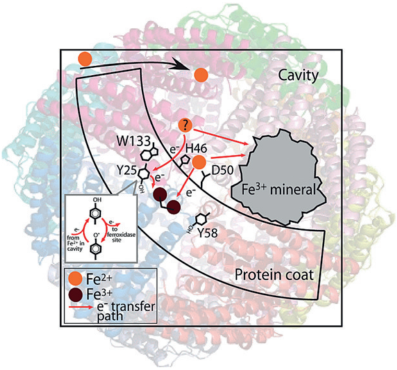

A radical view of bacterioferritin: Three aromatic residues located close to the catalytic ferroxidase site are shown to be important for iron mineralization. A transient radical is associated with Tyr25, consistent with a mechanism where electrons from Fe^{2+} oxidation are transferred to the oxidized, di-Fe^{3+} ferroxidase site, ensuring that two electrons arrive at the site simultaneously and avoid formation of toxic reactive oxygen species.

Imaging Agents

R. Kojima, H. Takakura, M. Kamiya,
E. Kobayashi, T. Komatsu, T. Ueno,
T. Terai, K. Hanaoka, T. Nagano,
Y. Urano* ______ **14768 – 14771**

Development of a Sensitive Bioluminogenic Probe for Imaging Highly Reactive Oxygen Species in Living Rats

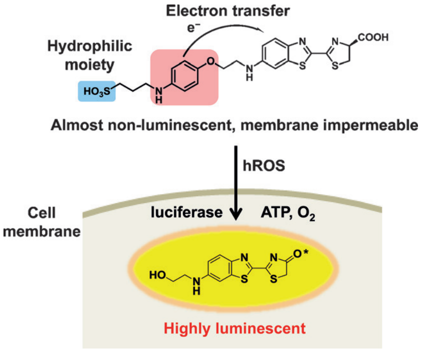

You light up my life: A sensitive bioluminogenic probe for highly reactive oxygen species (hROS) was developed based on the concept of dual control of bioluminescence emission by means of bioluminescent enzyme-induced electron transfer (BioLeT) and modulation of cell-membrane permeability. This probe enables non-invasive visualization of physiologically relevant amounts of hROS generated deep inside the body of living rats.

Femtochemistry

J. W. Ho, H. C. Yen, H. Q. Shi,
L. H. Cheng, C. N. Weng, W. K. Chou,
C. C. Chiu, P. Y. Cheng* **14772–14776**

Microhydration Effects on the Ultrafast Photodynamics of Cytosine: Evidences for a Possible Hydration-Site Dependence

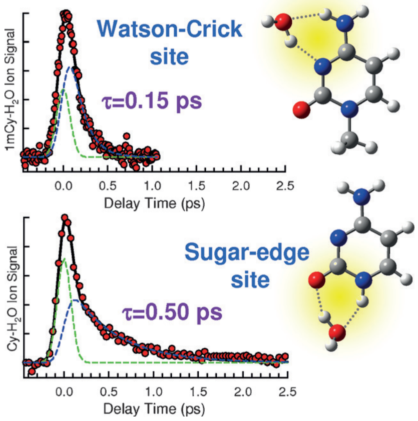

Hydration-site dependence: The ultrafast excited-state deactivation dynamics of small cytosine microhydrates produced in a supersonic expansion was studied by mass-selected femtosecond pump–probe photoionization spectroscopy. The results suggest that monohydration of cytosine at the amino Watson–Crick site induces a substantially stronger effect on the deaktivation than at the sugar-edge site in accelerating the excited-state deactivation.

Spin Transition Complexes

T. Romero-Morcillo, M. Seredyuk,*
M. C. Muñoz, J. A. Real* **14777–14781**

Meltable Spin Transition Molecular Materials with Tunable T_c and Hysteresis Loop Width

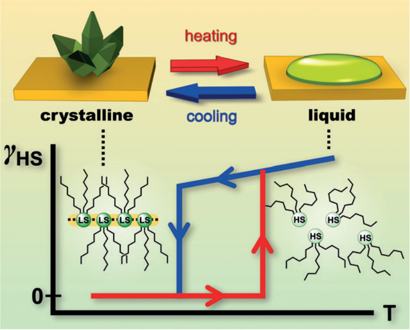

Soft matter? Doesn't matter! Abrupt high spin-to-low spin transition with controllable transition temperature and hysteresis width is achieved in soft-matter Fe^{II} meltable complexes.

Lithium-Ion Batteries

L. Zhou, M. Leskes, T. Liu,
C. P. Grey* **14782–14786**

Probing Dynamic Processes in Lithium-Ion Batteries by In Situ NMR Spectroscopy: Application to $Li_{1.08}Mn_{1.92}O_4$ Electrodes

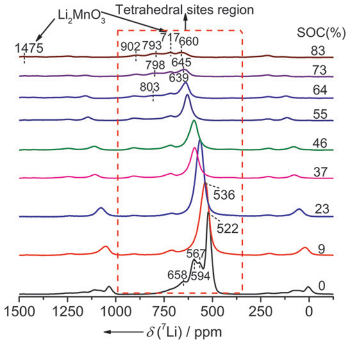

Mobi-Li-ty: Lithium mobility, as a function of temperature during battery cycling, can be simply monitored by using in situ T_2' relaxation measurements. Since Li dynamics are strongly related to structural properties, the changes in in situ T_2' can be used to detect structural changes, such as Li ordering.

Perovskite Defects

D. Batuk, M. Batuk, A. A. Tsirlin,
J. Hadermann,
A. M. Abakumov* **14787–14790**

Trapping of Oxygen Vacancies at Crystallographic Shear Planes in Acceptor-Doped Pb-Based Ferroelectrics

All lined up: In the ferroelectric material $PbTiO_3$, the substitution of Ti^{IV} by Fe^{III} leads to a segregation of the point oxygen vacancies into crystallographic shear (CS) planes, observed already at a vacancy concentration of about 1.7%. The CS planes occur as random planar defects at low Fe^{III} doping and demonstrate long-range order when the Fe^{III} concentration rises above circa 20 atom%.

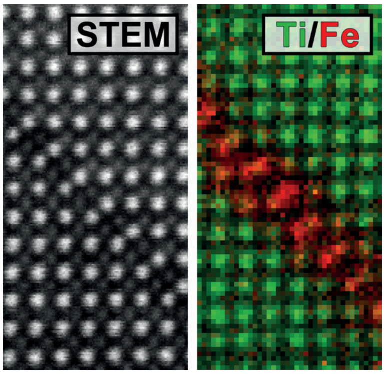

Host–Guest Chemistry

T. Futagoishi, M. Murata, A. Wakamiya,
Y. Murata* ______ **14791 – 14794**

Trapping N_2 and CO_2 on the Sub-Nano Scale in the Confined Internal Spaces of Open-Cage C_{60} Derivatives: Isolation and Structural Characterization of the Host–Guest Complexes

Single-molecule trap: After insertion of N_2 and CO_2 molecules into open-cage C_{60} tetraketone, a subsequent selective reduction of one of the four carbonyl groups induced a contraction of the opening and trapped the guest molecules. The isolation of the thus obtained molecular complexes was accomplished by recycling HPLC. These structures were unambiguously determined by single-crystal X-ray analyses.

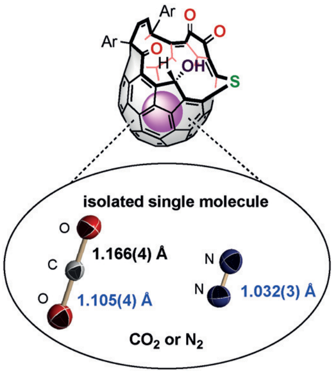

Protonation

S. Banerjee, R. N. Zare* _ **14795 – 14799**

Syntheses of Isoquinoline and Substituted Quinolines in Charged Microdroplets

Microdroplet chemistry: Isoquinolines and quinolines can be synthesized in charged microdroplets during a flight time on the order of a few milliseconds without the addition of external acid as a catalyst. The surface characteristics of the microdroplet are shown to play a critical role in accomplishing these reactions at enhanced rates.

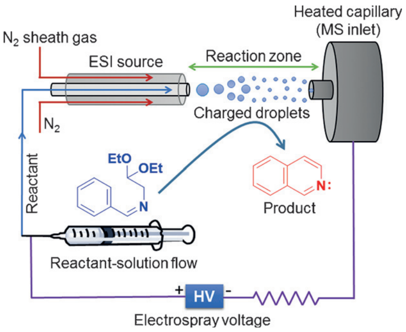

Membranes

N. Moridi, P. F.-X. Corvini,
P. Shahgaldian* ______ **14800 – 14804**

Reversible Supramolecular Surface Attachment of Enzyme–Polymer Conjugates for the Design of Biocatalytic Filtration Membranes

Inside Back Cover

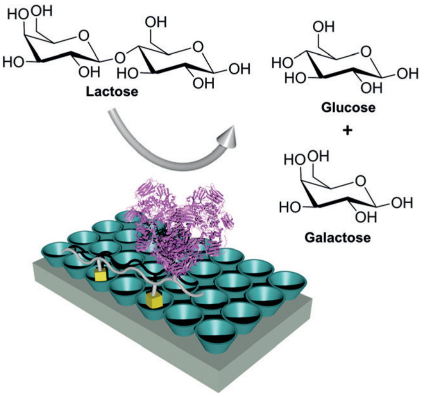

Enzyme in the membrane: Supramolecular and reversible surface bioconjugation on a filtration membrane is achieved using a new enzyme–polymer conjugate containing multiple adamantyl units. As part of a membrane bioreactor this supramolecular modification is stable under operational conditions and allows for efficient biocatalysis.

Metal-Free Catalysis

D. W. Kim, S. Joung,* J. G. Kim,*
S. Chang* ______ **14805 – 14809**

Metal-Free Hydrosilylation Polymerization by Borane Catalyst

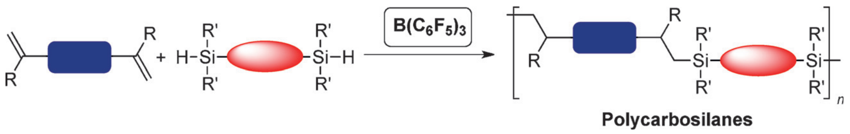

The borane supremacy: The first example of metal-free hydrosilylation polymerization between dienes and disilanes is developed by using a borane catalyst, $B(C_6F_5)_3$ to replace precious-metal-based systems. Under the easy-to-handle and mild conditions, various combinations of dienes and disilanes produced polycarbosilanes with a broad range of structures and properties.

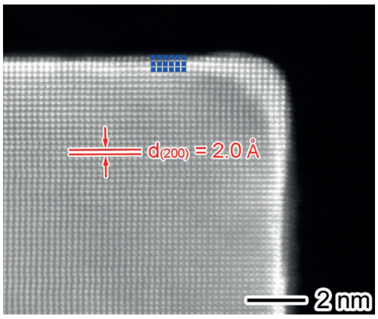

Atomically controlled Pd@Pt quasi-core–shell cocatalysts have been designed and used in combination with TiO$_2$ nanosheets as a model semiconductor for photocatalysis. The three-atom-thick Pt shell significantly enhances charge separation and water activation, which leads to a dramatically improved water splitting efficiency.

Water Splitting

S. Bai, L. Yang, C. Wang, Y. Lin, J. Lu, J. Jiang, Y. Xiong* ______ **14810 – 14814**

Boosting Photocatalytic Water Splitting: Interfacial Charge Polarization in Atomically Controlled Core–Shell Cocatalysts

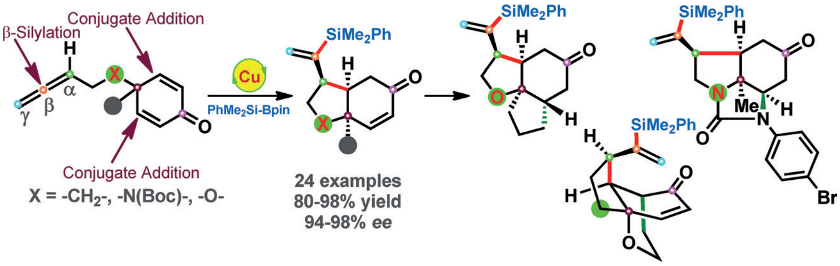

Three in one: Three consecutive chiral carbon centers are formed in one step by a copper-catalyzed asymmetric silylative cyclization of cyclohexadienone-tethered allenes. Thus *cis*-hydrobenzofuran, *cis*-hydroindole, and *cis*-hydroindene frameworks are prepared with exceptional yields (80–98 %) and enantioselectivities (94–98 % *ee*).

Asymmetric Synthesis

Z.-T. He, X.-Q. Tang, L.-B. Xie, M. Cheng, P. Tian,* G.-Q. Lin ______ **14815 – 14818**

Efficient Access to Bicyclo[4.3.0]nonanes: Copper-Catalyzed Asymmetric Silylative Cyclization of Cyclohexadienone-Tethered Allenes

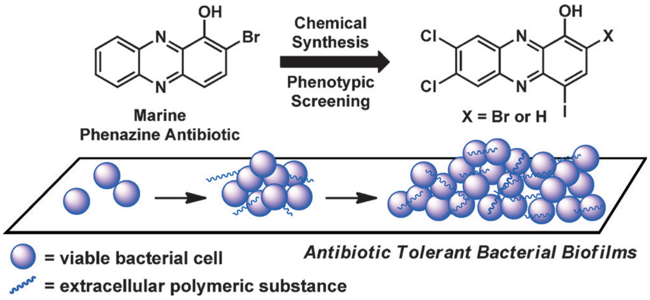

Killing the quiet bacteria: Biofilms and quiescent persister cells are typically resistant to standard antibiotics, and contribute to many human infections. Halogenated phenazines based on a marine natural product are shown to be potent anti-biofilm and anti-persister cell compounds, while displaying very limited cytotoxicity in mammalian cells.

Antibiofilm Compounds

A. T. Garrison, Y. Abouelhassan, D. Kallifidas, F. Bai, M. Ukhanova, V. Mai, S. Jin, H. Luesch, R. W. Huigens, III* ______ **14819 – 14823**

Halogenated Phenazines that Potently Eradicate Biofilms, MRSA Persister Cells in Non-Biofilm Cultures, and *Mycobacterium tuberculosis*

Catalytic H_2 Production

T.-W. Chiou,* T.-T. Lu,* Y.-H. Wu, Y.-J. Yu, L.-K. Chu, W.-F. Liaw* ____ **14824 – 14829**

Development of a Dinitrosyl Iron Complex Molecular Catalyst into a Hydrogen Evolution Cathode

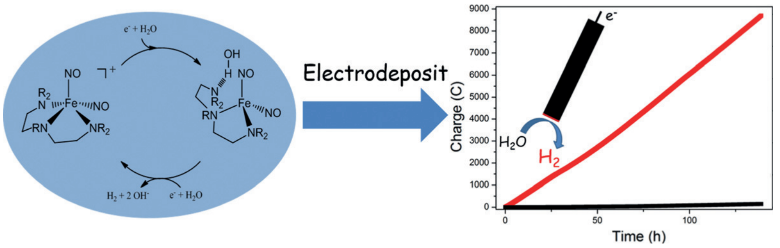

From complex to cathode: Dinitrosyl iron complex-deposited electrodes feature smaller Tafel slope than platinum electrodes in 1 м KCl, as well as exceptional longevity for electrocatalytic H_2-generation. This approach opens the door for adapting other molecular catalysts into solid-state cathodes.

Supramolecular Polymers

K. Kinjo, T. Hirao, S. Kihara, Y. Katsumoto, T. Haino* ____ **14830 – 14834**

Supramolecular Porphyrin Copolymer Assembled through Host–Guest Interactions and Metal–Ligand Coordination

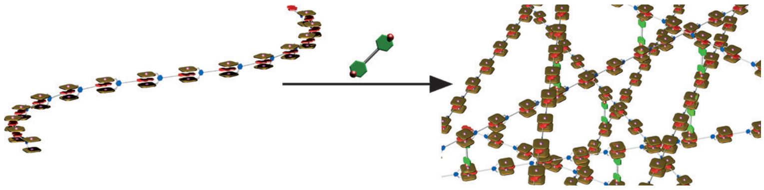

A zinc bisporphyrin cleft molecule possessing a guest moiety assembled through host-guest interactions to form supramolecular porphyrin polymers that were cross-linked by bispyridine-coordination. The resulting cross-linked polymers were entangled in solution, and a free-standing film was fabricated with a Young's modulus of 1 GPa.

cis-Bimetalloporphycene

T. Sarma, B. S. Kumar, P. K. Panda* ____ **14835 – 14839**

β,β′-Bipyrrole Fusion-Driven *cis*-Bimetallic Complexation in Isomeric Porphyrin

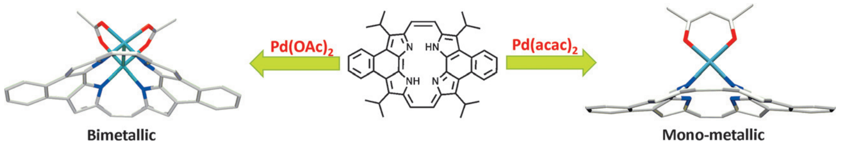

A *cis*-dipalladium complex of dinaphthoporphycene (DNP) is reported, coordinating two metals on the same side of the macrocycle. Replacement of the bridging ligand leads to an unsymmetrical mono Pd sitting atop complex, where DNP acts as a bidentate ligand.

Gels

A. Singh, B. A. Lindquist, G. K. Ong, R. B. Jadrich, A. Singh, H. Ha, C. J. Ellison, T. M. Truskett,* D. J. Milliron* ____ **14840 – 14844**

Linking Semiconductor Nanocrystals into Gel Networks through All-Inorganic Bridges

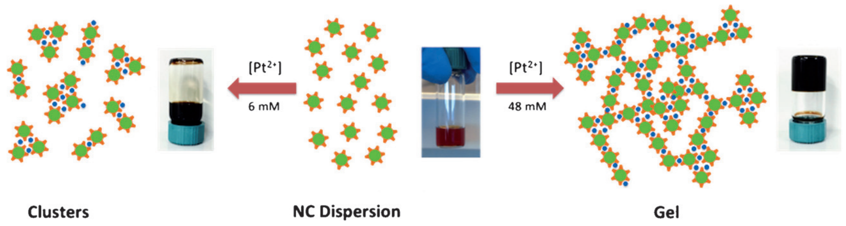

To cap it all: Capping inorganic nanocrystals (NCs) with chalcogenidometallate clusters allows the chalcogenidometallate clusters to act as anchors for coordinating metal ions. Pt^{2+} ions can bind to the clusters and act as linkers by forming coordination bonds. Depending on Pt^{2+} ion concentration the linked chalcogenidometallate-capped NCs can form all-inorganic gel networks.

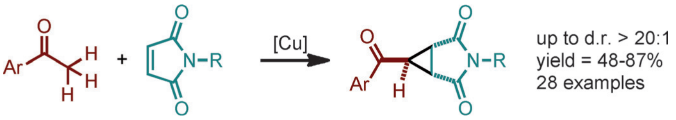

A practical synthesis of azabicyclo[3.1.0]hexane derivatives by direct oxidative coupling of arylmethyl ketones and maleimides was developed. The dehydrogenative annulation involves a double C−H bond functionalization at the α-position of the ketone using a copper(II) complex as the catalyst and di-*tert*-butyl peroxide as the oxidant.

Small-Ring Compounds

S. Manna,
A. P. Antonchick* ______ **14845 – 14848**

Copper-Catalyzed (2+1) Annulation of Acetophenones with Maleimides: Direct Synthesis of Cyclopropanes

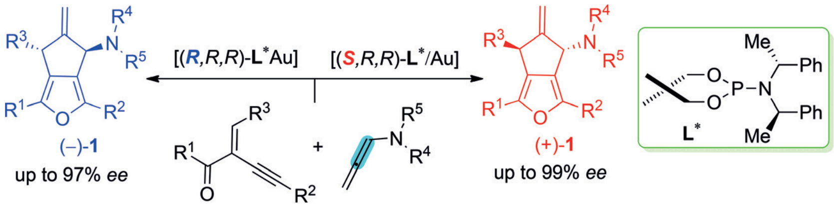

On the double: An unprecedented [3+2] annulation takes place with the proximal C=C bond of N-allenamides in the presence of a chiral gold catalyst. Both enantiomers could be obtained in good yields with high regio-, diastereo-, and enantioselectivities by using either diastereomer of a binol-derived phosphoramidite ligand. binol = 1,1′-bi-2-naphthol.

Cycloaddition

Y. Wang, P. Zhang, D. Qian,
J. Zhang* ______ **14849 – 14852**

Highly Regio-, Diastereo-, and Enantioselective Gold(I)-Catalyzed Intermolecular Annulations with N-Allenamides at the Proximal C=C Bond

Back Cover

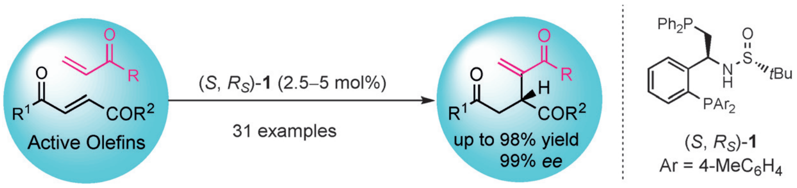

Highly efficient chiral sulfinamide bisphosphine catalysts (Wei-Phos, **1**) were developed that could be easily prepared from commercially available starting materials. Wei-Phos has shown good performance in the intermolecular cross-Rauhut–Currier reactions of vinyl ketones and 3-acyl acrylates or 2-ene-1,4-diones, leading to products in high yields with up to 99% *ee* under 2.5–5.0 mol% catalyst loading.

Asymmetric Catalysis

W. Zhou, X. Su, M. Tao, C. Zhu, Q. Zhao,*
J. Zhang* ______ **14853 – 14857**

Chiral Sulfinamide Bisphosphine Catalysts: Design, Synthesis, and Application in Highly Enantioselective Intermolecular Cross-Rauhut–Currier Reactions

The importance of being (diastereomerically) earnest: Chiral 2,2′-bipyrrolidine-based salan ligands give Al complexes as single diastereomers, which are active catalysts for stereoselective polymerization of racemic lactide. The heterotacticity of the obtained poly(lactic acid) increased dramatically upon increasing the enantiomeric impurity of the catalyst as the result of an insertion/auto-inhibition/exchange mechanism.

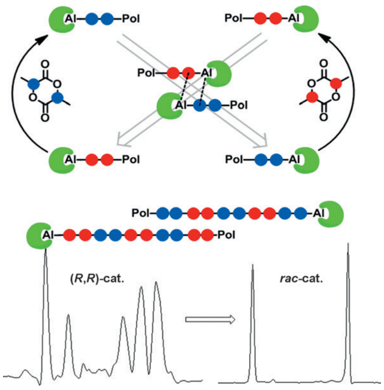

Diastereoselectivity

K. Press, I. Goldberg,
M. Kol* ______ **14858 – 14861**

Mechanistic Insight into the Stereochemical Control of Lactide Polymerization by Salan–Aluminum Catalysts

Photovoltaic Devices

B. Yang, O. Dyck, J. Poplawsky, J. Keum, S. Das, A. Puretzky, T. Aytug, P. C. Joshi, C. M. Rouleau, G. Duscher, D. B. Geohegan, K. Xiao* **14862 – 14865**

Controllable Growth of Perovskite Films by Room-Temperature Air Exposure for Efficient Planar Heterojunction Photovoltaic Cells

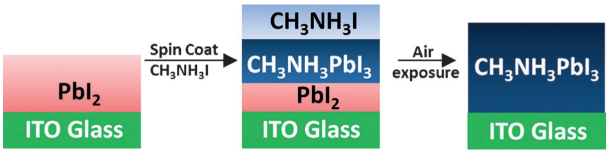

A breath of fresh air: Simple room-temperature air exposure can drive the interdiffusion between perovskite precursor layers and crystallize the perovskite thin films. The obtained perovskite films show high crystallinity and well-aligned orientation. The devices with and without a TiO_2 electron transporting layer yielded high efficiencies of 15.6 % and 13.8 %, respectively.

Hydroarylation

G. E. M. Crisenza, O. O. Sokolova, J. F. Bower* **14866 – 14870**

Branch-Selective Alkene Hydroarylation by Cooperative Destabilization: Iridium-Catalyzed *ortho*-Alkylation of Acetanilides

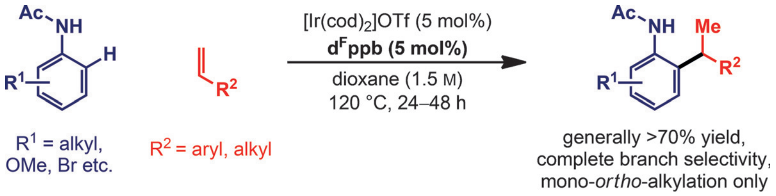

An iridium(I) catalyst system modified with the wide-bite-angle and electron-deficient bisphosphine d^{F}ppb (1,4-bis(di(pentafluorophenyl)phosphino)butane) promotes highly branch-selective hydroarylation reactions between diverse acetanilides and aryl- or alkyl-substituted alkenes. This provides direct and *ortho*-selective access to synthetically challenging anilines.

Ruthenium Silane Complexes

M. Nagaoka, H. Tsuruda, M.-a. Amako, H. Suzuki, T. Takao* **14871 – 14874**

μ_3-η^2:η^2:η^2-Coordination of Primary Silane on a Triruthenium Plane

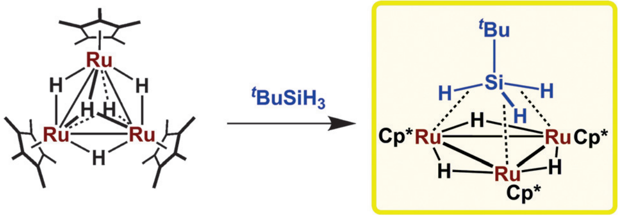

Silane on a plane: The reaction of [{Cp*Ru(μ-H)}$_3$(μ$_3$-H)$_2$] with *t*BuSiH$_3$ afforded a μ$_3$-silane complex in which primary silane coordinates to the triruthenium plane while maintaining three Si–H interactions. The unique μ_3-η^2:η^2:η^2-coordination can be regarded as an arrested intermediate of oxidative addition of a primary silane to the trinuclear site as well as a model for the chemisorption of saturated compounds on a metal surface.

Cross-Coupling

G. Pandey,* R. Laha **14875 – 14879**

Visible-Light-Catalyzed Direct Benzylic C(sp^3)–H Amination Reaction by Cross-Dehydrogenative Coupling

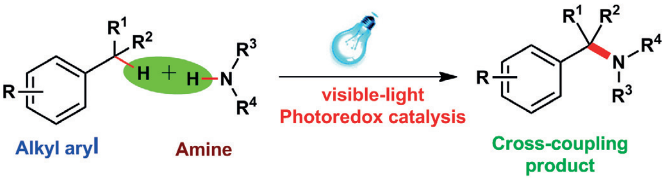

Amination: A metal and external oxidant-free benzylic amination driven by visible light in the presence of a sensitizer is reported (see picture). This approach is an innovative addition to the established procedures. The substrate scope and mechanistic experiments provide a good insight into the general reaction.

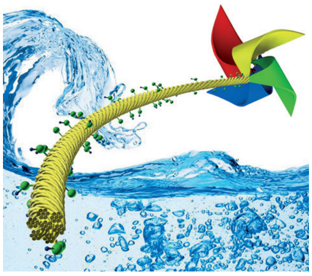

Water lot of twisting: Hydrophilic, hierarchically helical carbon-nanotube fibers are synthesized. In response to water and moisture they rapidly contract and rotate. The large numbers of nano- and micron-scale channels are responsible for these moisture-sensing properties. The fibers are lightweight, flexible, and strong, making them suitable for applications, such as smart switches, actuators, robots, and biomimetic devices.

Actuators

S. He, P. Chen, L. Qiu, B. Wang, X. Sun, Y. Xu, H. Peng* ______ **14880 – 14884**

A Mechanically Actuating Carbon-Nanotube Fiber in Response to Water and Moisture

---

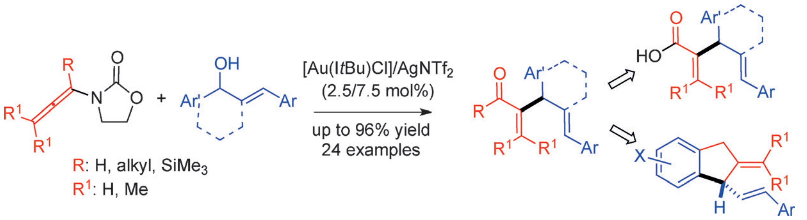

A golden ally in allylation: In a gold(I)-assisted formal α-allylation of acrylaldehyde, enones, and acyl silanes with alcohols, allenamides were used as precursors to intermediate α-gold-substituted unsaturated carbonyl compounds. The transformation enabled the synthesis of a diverse range of products under mild conditions (see scheme; I*t*Bu = 1,3-di(*tert*-butyl)imidazol-2-ylidene).

Homogeneous Catalysis

M. M. Mastandrea, N. Mellonie, P. Giacinto, A. Collado, S. P. Nolan, G. P. Miscione, A. Bottoni, M. Bandini* ______ **14885 – 14889**

Gold(I)-Assisted α-Allylation of Enals and Enones with Alcohols

---

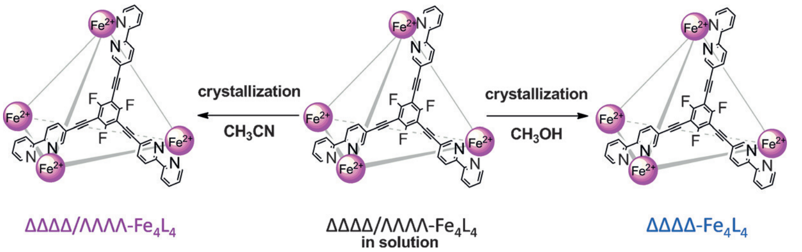

Supramolecular chiral resolution: A highly electron-deficient tetrahedral cage was formed from a stable tris(bipyridyl) ligand and a Fe^{II} salt. Crystallization of the racemic CH_3OH solution leads to spontaneous resolution of the cages, whereas crystallization from CH_3CN does not. The encapsulation of an anionic guest was observed in CH_3CN.

Cage Complexes

P. Bonakdarzadeh, F. Pan, E. Kalenius, O. Jurček, K. Rissanen* ______ **14890 – 14893**

Spontaneous Resolution of an Electron-Deficient Tetrahedral Fe_4L_4 cage

---

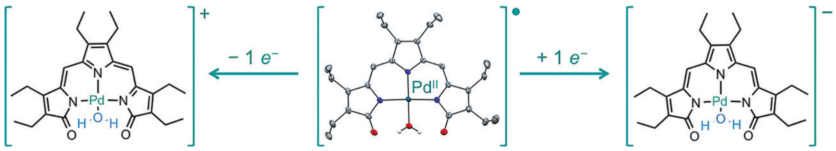

The positive, the negative, and the radical: The tripyrrin-1,14-dione scaffold of urinary pigment uroerythrin coordinates divalent palladium as a planar tridentate ligand. The resulting complex presents a ligand-based radical and is stable at room temperature. One-electron oxidation and reduction reactions lead to the characterization of a series of three Pd^{II} complexes featuring this ligand framework in three redox states.

Non-Innocent Ligands

R. Gautam, J. J. Loughrey, A. V. Astashkin, J. Shearer, E. Tomat* ______ **14894 – 14897**

Tripyrrindione as a Redox-Active Ligand: Palladium(II) Coordination in Three Redox States

Photocatalysis

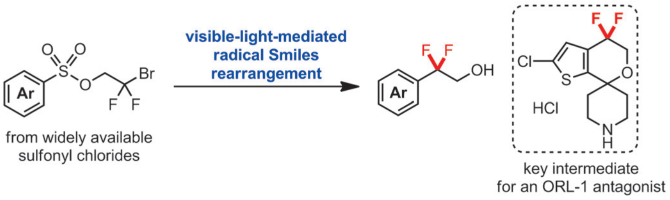

A reason for Smiles: A visible-light-mediated radical Smiles rearrangement addresses the challenging synthesis of the *gem*-difluoro group present in an opioid receptor-like 1 (ORL-1) antagonist and enables the introduction of the difluoroethanol motif into a range of aryl and heteroaryl systems. When applied to the target compound, the photochemical step could be conducted on 15 g scale at a $[Ru(bpy)_3]Cl_2$ loading of 0.01 mol%.

Ionic Liquids

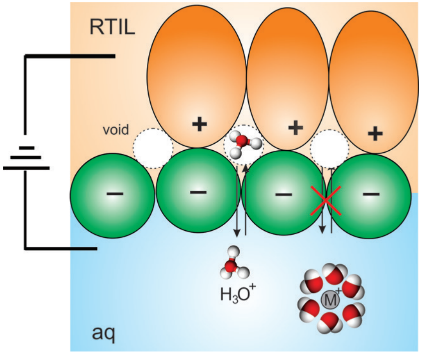

Protons squeezing through the interface: At the water/ionic liquid interface, size-dependent transfer of protons into voids of the ionic liquid phase occurs with electrochemical control. These results can have implications in a variety of proton transfer reactions, such as in fuel cells and hydrogen storage.

Amine Oxidation

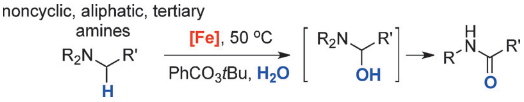

Let's iron it out! The title reaction enables the oxidative synthesis of amides directly from tertiary, noncyclic alkyl amines under synthetically useful, mild conditions through a biologically inspired approach employing oxidative iron catalysis. Mechanistic studies suggest that hemiaminals are likely intermediates in this reaction and that the catalytic system can be employed for other C_α–H oxidations of amines.

Fluorination

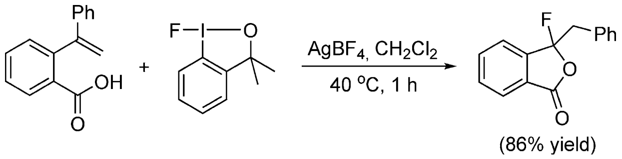

All in one: A new class of lactones containing a tertiary alkyl fluoride was prepared in high yields by using a stable fluoroiodane reagent. This unique reaction incorporates a cyclization, an aryl migration, and a fluorination all in one step.

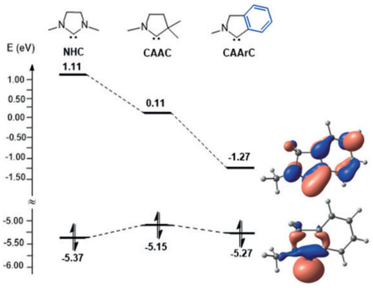

CAArC: The replacement of the alkyl substituent of cyclic (alkyl)(amino)-carbenes (CAACs) by aryl scaffolds not only enhances the π-accepting properties of the carbene center, but also retains the strong σ-donating properties of CAACs, leading to a small singlet–triplet gap. Despite the instability of CAArCs, the corresponding transition-metal complexes are readily available, and they appear to be efficient catalysts for several chemical transformations.

N-Heterocyclic Carbenes

B. Rao, H. Tang, X. Zeng,* L. Liu,
M. Melaimi, G. Bertrand* **14915 – 14919**

Cyclic (Amino)(aryl)carbenes (CAArCs) as Strong σ-Donating and π-Accepting Ligands for Transition Metals

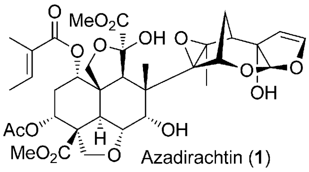

Azadirachtin (**1**)

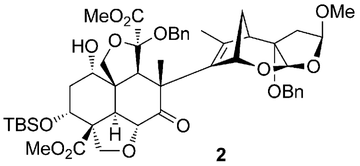

2

The asymmetric formal synthesis of azadirachtin (**1**) was accomplished by utilizing the tandem radical cyclization reaction as a key step. The route to the key intermediate **2** requires the longest linear sequence of 30 steps.

Natural Product Synthesis

N. Mori, T. Kitahara, K. Mori,
H. Watanabe* **14920 – 14923**

Asymmetric Formal Synthesis of Azadirachtin

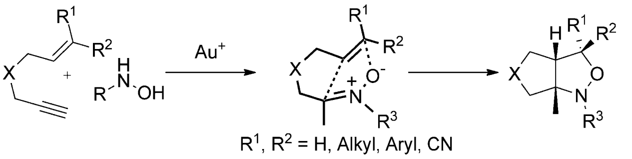

R^1, R^2 = H, Alkyl, Aryl, CN
X = O, NTs

Kinetically unstable nitrones are generated from gold-catalyzed reactions of 1,6-enynes with *N*-hydroxyanilines, and subsequently trapped by tethered alkenes to furnish [2+2+1]-annulations. These findings open the door to new ways to access ketone nitrones with good stereoselectivity.

Enyne Annulation

D. B. Huple, B. D. Mokar,
R.-S. Liu* **14924 – 14928**

Alkene-Directed *N*-Attack Chemoselectivity in the Gold-Catalyzed [2+2+1]-Annulations of 1,6-Enynes with *N*-Hydroxyanilines

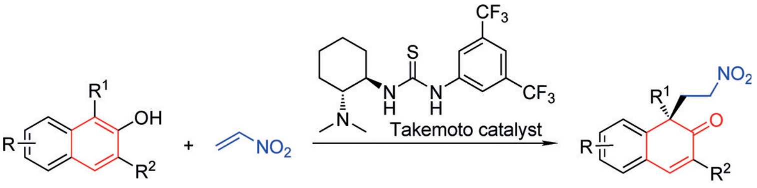

An intermolecular asymmetric dearomatization reaction of β-naphthols with nitroethylene through a chiral-thiourea-catalyzed Michael reaction is described. Enantioenriched functionalized β-naphthalenones with an all-carbon quaternary stereogenic center were easily constructed in good yields and excellent enantioselectivity (up to 79% yield, 98% *ee*).

Organocatalysis

S.-G. Wang, X.-J. Liu, Q.-C. Zhao,
C. Zheng, S.-B. Wang,
S.-L. You* **14929 – 14932**

Asymmetric Dearomatization of β-Naphthols through a Bifunctional-Thiourea-Catalyzed Michael Reaction

Lanthanide Spectroscopy

T. Wu,* J. Kapitán,* V. Mašek,
P. Bouř* ______ 14933 – 14936

Detection of Circularly Polarized Luminescence of a Cs-Eu^{III} Complex in Raman Optical Activity Experiments

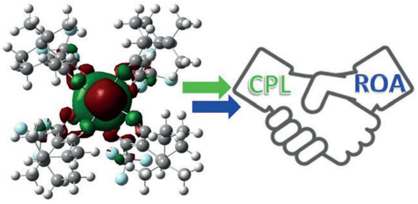

A cesium–europium complex displayed strong circularly polarized luminescence (CPL) that could be recorded using Raman optical activity (ROA) spectroscopy. The sensitivity and unique features of the resulting spectra indicate that ROA is generally applicable for chiral lanthanide labels.

Natural Product Synthesis

Z. Xu, X. Bao, Q. Wang,
J. Zhu* ______ 14937 – 14940

An Enantioselective Total Synthesis of (−)-Isoschizogamine

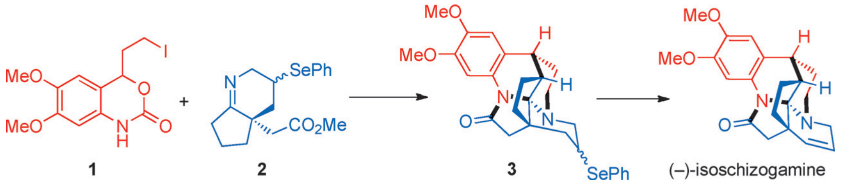

Mix and go: Simply heating the alkyl iodide **1** and imine **2** afforded the hexacyclic compound **3**, which was subsequently converted, in one step, into (−)-isoschizogamine. Pivalic acid is the only reagent needed to promote this complex yet ordered domino sequence creating three rings and three contiguous stereogenic centers with complete control of both the relative and absolute stereochemistry.

Carbenes

S. Lv, J. Wang, C. Zhang, S. Xu, M. Shi,
J. Zhang* ______ 14941 – 14946

Silver-Catalyzed Amidiniumation of Alkynes: Isolation of a Silver Intermediate, Synthesis of Enamine Amido Carbene Precursors, and an Unprecedented Umpolung of Propiolamide

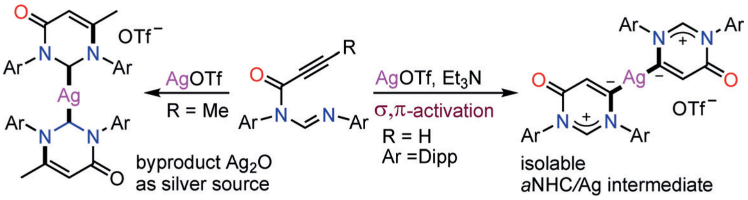

Having effects: The title reaction has been developed for the synthesis of carbene precursors, including the isolation of a novel silver intermediate. Control experiments reveal the unexpected effects of both HOTf and substrate substituents on the silver-activation mode and the cyclization process.

Graphene Fibers

T. Chen, L. Dai* ______ 14947 – 14950

Macroscopic Graphene Fibers Directly Assembled from CVD-Grown Fiber-Shaped Hollow Graphene Tubes

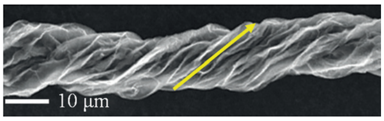

Down to the wire: Multilayer graphene tubes can be grown by CVD on a copper wire. Dissolving the copper wire leaves a free graphene tube that is as long as the wire used. This novel approach gives porous graphene fibers with high electrical conductivity and flexibility. A high efficiency fiber-shaped dye-sensitized solar cell was prepared by using these graphene fibers.

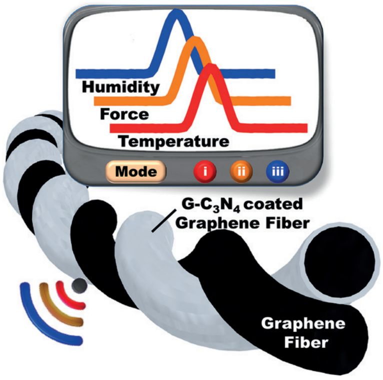

A fibriform environmental responsor is fabricated on double-helix graphene-based microfibers, and exhibits selective sensitivity towards tiny perturbations of temperature, mechanical force, and humidity. The responsor is capable of recognizing various types of stimuli, and therefore may find applications in environmental or human body monitoring devices.

Graphene Sensors

F. Zhao, Y. Zhao, H. Cheng, L. Qu* ———— **14951 – 14955**

A Graphene Fibriform Responsor for Sensing Heat, Humidity, and Mechanical Changes

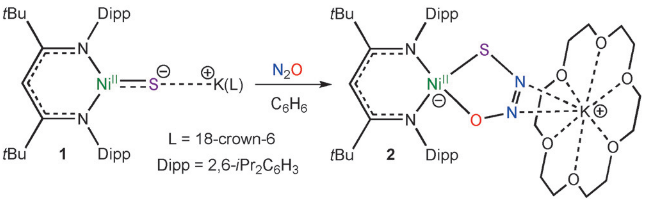

Late-metal sulfides: Reductive deprotection of β-diketiminate-supported nickel tritylthiolate complexes results in the formation of the first “masked” terminal nickel sulfide complexes. Surprisingly, **1** reacts with nitrous oxide (N_2O) in a [3+2] cycloaddition across the Ni−S bond to form an unprecedented *cis*-thiohyponitrite complex (**2**).

Coordination Chemistry

N. J. Hartmann, G. Wu, T. W. Hayton* ———— **14956 – 14959**

Synthesis of a “Masked” Terminal Nickel(II) Sulfide by Reductive Deprotection and its Reaction with Nitrous Oxide

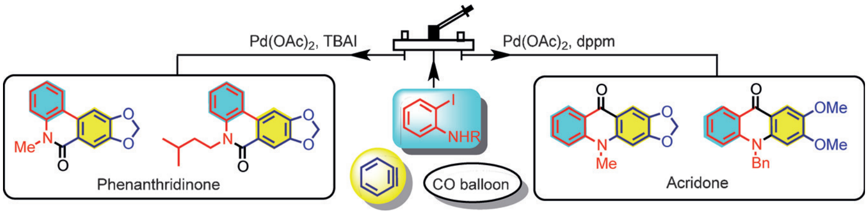

Divergent alkaloid synthesis: A multicomponent, regioselective approach for palladium-catalyzed C_1 insertion is described. This reaction was applied in the divergent synthesis of phenanthridinone and acridone natural product core scaffolds.

Aryne Insertion

M. Feng, B. Tang, N. Wang, H.-X. Xu, X. Jiang* ———— **14960 – 14964**

Ligand Controlled Regiodivergent C_1 Insertion on Arynes for Construction of Phenanthridinone and Acridone Alkaloids

Easy to handle: A new method for CF_3SO_2Na-based direct trifluoromethylthiolation of C(sp^2)−H bonds has been developed. CF_3SSCF_3 is generated in situ from cheap and easy-to-handle CF_3SO_2Na, and in the presence of CuCl can be used for electrophilic trifluoromethylthiolation of indoles, pyrroles, and enamines. The method has been extended to perfluoroalkylthiolation reactions using R_fSO_2Na.

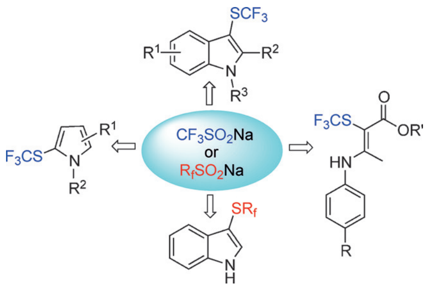

Heterocycle Synthesis

L. Jiang, J. Qian, W. Yi,* G. Lu, C. Cai, W. Zhang* ———— **14965 – 14969**

Direct Trifluoromethylthiolation and Perfluoroalkylthiolation of C(sp^2)−H Bonds with CF_3SO_2Na and R_fSO_2Na

Ionic Liquids

Borenium superacids: The solvent-free synthesis of ionic liquids based on borenium cations and chlorometalate anions afforded a new class of liquid Lewis superacids with Gutmann acceptor numbers of up to 182. The Lewis acidity was enhanced by the absence of a solvent, which was enabled by the ionic-liquid environment.

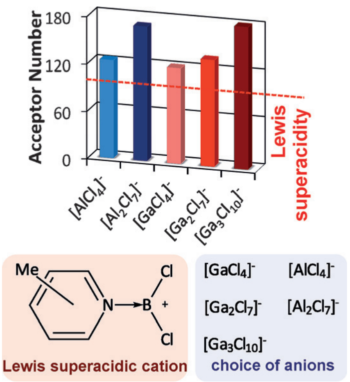

Spin-Forbidden Reactions

Forbidden or allowed? The four-electron oxidative addition of O_2 to $TpCr^I$ complexes (Tp = tris(pyrazolyl)borate) is spin-forbidden, and yet, it proceeds by a non-adiabatic crossing from a quartet to a doublet potential energy surface at the minimum-energy crossing point, the structure of which is shown.

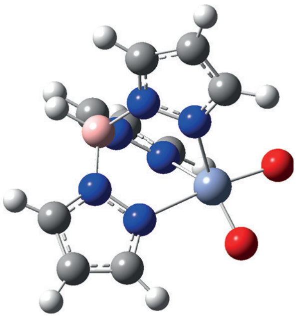

Supporting information is available on www.angewandte.org (see article for access details).

A video clip is available as Supporting Information on www.angewandte.org (see article for access details).

This article is available online free of charge (Open Access).

This article is accompanied by a cover picture (front or back cover, and inside or outside).

The Very Important Papers, marked VIP, have been rated unanimously as very important by the referees.

The Hot Papers are articles that the Editors have chosen on the basis of the referee reports to be of particular importance for an intensely studied area of research.